Active Black Holes: Relevant Plasma Structures, Regimes and Processes Involving All Phase Space

Bruno Coppi
Massachusetts Institute of Technology
Cambridge, MA 02139

Abstract. The presented theory is motivated by the growing body of experimental information on the characteristics, connected with relevant spectral, time and space resolutions, of the radiation emission from objects considered as rotating black holes. In the immediate surroundings of these objects three plasma regions are identified: an innermost Buffer Region, an intermediate Three-regime Region and a Structured Peripheral Region. In the last region a Composite Disk Structure made of a sequence of plasma rings corresponding to the formation of closed magnetic surfaces is considered to be present and to allow intermittent accretion flows along the relevant separatrices. The non-linear "Master Equation" describing composite disk structures is derived and solved in appropriate asymptotic limits. A ring configuration, depending on the state of the plasma at the microscopic level: i) can be excluded from forming given the strongly non-thermal nature of the electron distribution (in momentum space) within the Three-regime Region allowing the onset of a spiral structure. The observed High Frequency Quasi Periodic Oscillations (HFQPOs) are associated with these tridimensional structures; ii) may be allowed to propagate to the outer edge of the Buffer Region where successive rings carrying currents in opposite directions are ejected vertically (in opposite directions) and originate the observed jets; iii) penetrates in the Three-regime Region and is dissipated before reaching the outer edge of the Buffer Region. The absence of a coherent composite disk structure guiding accretion in the presence of a significant magnetic field background is suggested to characterize quiescent black holes.

I. Introduction

The advances made in the observation of the characteristics of the radiation emission [1,2,3] from compact objects and in particular from black hole candidates are an important incentive to attempt describing theoretically the plasmas surrounding these objects [4]. The spectral, time and spatial resolutions achieved from the analyses of these objects are precious guidelines for the theoretical plasma models that can be formulated. One of the purposes of this paper is to employ theoretical concepts and techniques developed in the investigation of magnetically confined laboratory plasmas to deal with the large variety of plasmas that can be associated with black holes and to make a connection with relevant experimental observations. Thus, coherent and stationary plasma and magnetic field configurations [5], collective modes that can be excited under realistic conditions [6] and characteristics of the plasma regimes [2,7] that can be produced around black holes are introduced and analyzed.

This paper is organized as follows. In Section II the basic equations that describe the equilibrium state of an axisymmetric plasma disk structure are derived. In Section III composite disk structures are identified and described on the basis of the Master Equation [8] for the relevant magnetic field configurations. The plasma pressure profiles that are associated with the relevant magnetic field configurations are derived. In Section IV the transition from the Core Region to the Envelope Region of the considered composite disk structures is analyzed. In Section V the theoretical issues that arise, when a radial accretion velocity [9,10,11] is present. In Section VI the Bursty Accretion process based on the onset of a ballooning instability [12,13] between adjacent current channels, containing close magnetic surfaces is proposed. In Section VII the effective gravitational potentials [14,15] that are used to include relevant effects of General Relativity in the analysis presented in the earlier sections are discussed. In Section VIII, the formation of three characteristic regions around black holes is envisioned and the onset of three regimes in the intermediate of these regions is proposed on the basis of existing experimental observations. These regimes are associated with three different magnetic field configurations on the basis of the analyses presented in the earlier sections. A set of concluding remarks is given in Section IX.

II. Basic Equations

We start our analysis with axisymmetric configurations for which the magnetic field is represented by

$$\mathbf{B} \simeq \frac{1}{R}\left[\nabla\psi \times \mathbf{e}_\phi + I(\psi, z)\mathbf{e}_\phi\right] \tag{1}$$

where we use cylindrical coordinates, $\mathbf{B}\cdot\nabla\psi = 0$, and $\psi(R, z) = \text{const.}$ represents the relevant magnetic surfaces. We consider at first the Newtonian limit where General Relativity corrections can be neglected. The plasma is rotating around a central object with a velocity

$$\mathrm{V}_\phi = R\Omega(R, z)$$

where [16]

$$\Omega(R, z) \simeq \Omega_k(R) + \delta\Omega(R, z)\ , \tag{2}$$

$\Omega_k \equiv \left(GM_*/R^3\right)^{1/2}$ is the Keplerian frequency for a central object of mass M_* and whose gravity is prevalent (that is, the plasma self gravity can be neglected) and $|\delta\Omega|/\Omega_k < 1$.

We assume that, in the grand scale, the hyperconductivity condition can be applied in the sense that

$$\mathbf{E}_\Omega + \frac{1}{c}\mathbf{V}\times\mathbf{B} = 0\ , \tag{3}$$

$\mathbf{E} = \mathbf{E}_\Omega + \Delta\mathbf{E}$,

$$-en\left[\Delta\mathbf{E} + \frac{1}{c}\left(\mathbf{u}_e - \Omega R\mathbf{e}_\phi\right)\times\mathbf{B}\right] - \nabla p_e - \alpha_T n\nabla T_e = 0\ , \tag{4}$$

where the last term represents the thermal force, the plasma resistivity is neglected and $\mathbf{u}_e$ is the (total) electron flow velocity. The corresponding equation for the ion population is, for $\rho = m_i n$,

$$-\rho\left(2R_0\Omega_k\delta\Omega + \frac{3z^2}{2R_0}\Omega_k^2\right)\mathbf{e}_R + en\Delta\mathbf{E} - \rho z\Omega_k^2\mathbf{e}_z - \nabla p_i + \alpha_T n\nabla T_e = 0\,. \tag{5}$$

Referring to Eq. (1) we note that the current density $\mathbf{J}$ is given by

$$\mathbf{J} = \frac{c}{4\pi}\nabla\times\mathbf{B} = -\frac{c}{4\pi R}\left[\left(\Delta_*\psi\right)\mathbf{e}_\phi - \nabla I\times\mathbf{e}_\phi\right], \tag{6}$$

where

$$\Delta_*\psi \equiv R\frac{\partial}{\partial R}\left(\frac{1}{R}\frac{\partial}{\partial R}\psi\right) + \frac{\partial^2}{\partial z^2}\psi\,, \tag{7}$$

and the magnetic force $\mathbf{F}_M$ by

$$\mathbf{F}_M = \frac{1}{c}\mathbf{J}\times\mathbf{B} = -\frac{1}{4\pi R^2}\left\{\left(\Delta_*\psi\right)\nabla\psi + I\nabla I - \left(\nabla I\times\nabla\psi\right)\mathbf{e}_\phi\right\}. \tag{8}$$

Clearly, if $I = I(\psi)$, $\nabla I = \left(dI/d\psi\right)\nabla\psi$ and $\mathbf{F}_M$ has no toroidal component.

This is the case that we shall consider and we may write $\mathbf{F}_M$ as

$$\mathbf{F}_M = -\frac{1}{4\pi}\left(G_\psi\right)\nabla\psi$$

where

$$G_\psi \equiv \frac{1}{R^2}\left(\Delta_*\psi + I\frac{d}{d\psi}I\right). \tag{9}$$

In the case of toroidal magnetically confined laboratory plasmas for which $\mathbf{F}_M = \nabla p$, $p = p_e + p_i$ being the plasma pressure, $\mathbf{B}\cdot\nabla p = 0$ and $p = p(\psi)$. Then

$$-\frac{1}{4\pi R^2}\left(\Delta_*\psi + I\frac{dI}{d\psi}\right) = \frac{dp}{d\psi} \tag{10}$$

is the well known equilibrium equation in the absence of a toroidal rotation velocity and, clearly,

$$\nabla\times\mathbf{F}_M = -\frac{1}{4\pi}\left(\nabla G_\psi\right)\times\nabla\psi = \left(\Delta\frac{dp}{d\psi}\right)\times\nabla\psi = 0\,. \tag{11}$$

In the case that we consider, the total momentum conservation equation that includes both the toroidal rotation velocity and the effect of the gravitational field due to a central object, is

$$-\rho\left(\Omega^2 R\mathbf{e}_R + \nabla\Phi_G\right) = -\nabla p + \frac{1}{c}\mathbf{J}\times\mathbf{B} \tag{12}$$

where

$$\Phi_G = \frac{GM_*}{\sqrt{R^2+z^2}}\,, \qquad \nabla\Phi_G \simeq -\frac{V_k^2}{R}\left(\mathbf{e}_R + \frac{z}{R}\mathbf{e}_z\right), \qquad V_k^2 \equiv \frac{GM_*}{R} \equiv \Omega_k^2 R^2\,.$$

Then we have

$$\mathbf{B}\cdot\nabla p=\rho R\left(\Omega^2-\Omega_k^2\right)B_R-z\rho\Omega_k^2B_z\neq 0 \tag{13}$$

and if we apply the $\nabla\times$ operator on Eq. (12) we obtain

$$\nabla\times\left(\rho\nabla\Phi_G+\rho\Omega^2R\mathbf{e}_R\right)$$

$$=\mathbf{e}_\phi\left\{\frac{\partial\rho}{\partial z}\left(R\Omega^2+\frac{\partial\Phi_G}{\partial R}\right)+\rho R2\Omega\frac{\partial\Omega}{\partial z}-\frac{\partial\rho}{\partial R}\frac{\partial\Phi_G}{\partial z}\right\}$$

$$=\frac{1}{4\pi}\left(\nabla G_\psi\right)\times\nabla\psi=\frac{1}{4\pi R^2}\left[-\frac{2}{R}\left(\Delta_*\psi+I\frac{dI}{d\psi}\right)\mathbf{e}_R+\nabla\left(\Delta_*\psi\right)\right]\times\nabla\psi\,. \tag{14}$$

Now, considering Eq. (2), Eq. (14) becomes

$$2\Omega_kR\frac{\partial}{\partial z}\left(\rho\delta\Omega\right)+z\Omega_k^2\left(\frac{\partial\rho}{\partial R}+\frac{3}{2}\frac{z}{R}\frac{\partial\rho}{\partial z}\right)$$

$$=\frac{1}{4\pi R^2}\left\{\left[\frac{2}{R}\left(\Delta_*\psi+I\frac{dI}{d\psi}\right)-\frac{\partial}{\partial R}\left(\Delta_*\psi\right)\right]\frac{\partial\psi}{\partial z}+\frac{\partial}{\partial z}\left(\Delta_*\psi\right)\frac{\partial\psi}{\partial R}\right\} \tag{15}$$

and we call it the "Master Equation".

In order to proceed further we consider a radial interval $\left|R-R_0\right|<R_0$ around a given radius R_0. Then

$$\Omega\simeq\Omega_k\left(R_0\right)+\left(R-R_0\right)\left.\frac{d\Omega_k}{dR}\right|_{R=R_0}+\delta\Omega \tag{16}$$

and we comply with the isorotation condition $\Omega=\Omega\left(\psi\right)$ defining ψ_z/ψ_{0k} by

$$\left(R-R_0\right)\left.\frac{d\Omega_k}{dR}\right|_{R=R_0}=\Omega_k^0\frac{\psi_z}{\psi_{0k}} \tag{17}$$

and ψ_1/B_0 by

$$2\Omega R\delta\Omega\simeq 2\Omega_k^0\left.\frac{d\Omega_k}{dR}\right|_{R=R_0}\frac{\psi_1}{B_0}=-\Omega_D^2\frac{\psi_1}{B_0R_0}\,, \tag{18}$$

where $\Omega_D^2\equiv-Rd\,\Omega^2/dR^2=3\Omega_k^2$ is considered to be the "driving factor" [6] for the onset of the magnetic configurations that are analyzed and $\left|\psi_1/\left(B_0R_0\right)^2\right|<1$.

We note that the vertical momentum conservation equation is

$$0\simeq-\frac{\partial p}{\partial z}-z\rho\Omega_k^2-\frac{1}{4\pi}G_\psi\frac{\partial\psi}{\partial z}\,, \tag{19}$$

that, given Eq. (9), becomes

$$0=-\frac{\partial p}{\partial z}-z\rho\Omega_k^2-\frac{1}{4\pi R^2}\frac{\partial\psi}{\partial z}\left(\Delta_*\psi+I\frac{dI}{d\psi}\right). \tag{20}$$

Clearly, we have two equations, (14) and (20), which give $\psi\left(R,z\right)$ and $p\left(R,z\right)$ for reasonable choices of $\delta\Omega\left(\psi_1\right)$, the density $\rho\left(R,z\right)$ and the poloidal current function $I\left(\psi\right)$. In particular, the choices for $\delta\Omega$ and $I\left(\psi\right)$ have to be guided

primarily by the criterion that the temperature $2T = pm_i/\rho$ have a realistic spatial profile with both p and ρ positive and $\rho\left(R,\, z^2/\Delta_z^2 \to \infty\right) \ll \rho\left(R,\, z^2/\Delta_z^2 \to 0\right)$ where Δ_z represents the scale distance over which the considered ring structure is localized. Clearly, p and ρ are taken as even functions of z while ψ_1 is an odd function of z.

We observe that a similar procedure was adopted when deriving, for the first time, the magnetic surface equation for the plasma in the immediate surroundings of a rotating neutron star [18] that is within the speed of light cylinder. In fact, this equation became known later as the "pulsar equation".

We shall consider peaked density profiles that are localized over a height about $4\Delta_z$ and are represented by

$$\rho_* = \bar{\rho}\left(R_*\right)\exp\left(-\frac{z^2}{2\Delta_z^2}\right) \tag{21}$$

where $R_* = \left(R - R_0\right)/\delta_R$, $\delta_R \ll R_0$, and $\bar{\rho}\left(R_*\right)$ is an even, periodic function of R_* representing a sequence of concentric plasma rings. In addition to this, broader profiles $\rho_G\left(R_*\right)$ corresponding to the "envelope" region have to be included. Then we separate the flux function ψ_1 into two components

$$\psi_1 = \psi_* + \psi_G \tag{22}$$

of which ψ_* is localized over the distance Δ_z and ψ_G is about independent of z over this distance. That is

$$\psi_* = \bar{\psi}_*\left(R_*\right)\exp\left(-\frac{z^2}{2\Delta_z^2}\right), \tag{23}$$

$$\psi_G = \bar{\psi}_G\left(R_*\right), \tag{24}$$

where $\bar{\psi}_*\left(R_*\right)$ and $\bar{\psi}_G\left(R_*\right)$ are odd, periodic functions of R_*. For the sake of simplicity, we take

$$I \simeq \frac{dI}{d\psi}\left(\psi_1 + \psi_z\right) \equiv \frac{I_0'}{\delta_R}\left(\psi_1 + \psi_z\right). \tag{25}$$

Then if we write

$$p = \bar{p}_{**}\left(R_*\right)\exp\left(-\frac{z^2}{\Delta_z^2}\right) + \bar{p}_G\left(R_*\right)\exp\left(-\frac{z^2}{2\Delta_z^2}\right), \tag{26}$$

Eq. (20) can be split into the following two equations

$$0 = 2\bar{p}_{**} + \frac{1}{4\pi R^2\delta_R^2}\bar{\psi}_*\left[\frac{d^2}{dR_*^2}\bar{\psi}_* + \left(I_0'\right)^2\bar{\psi}_*\right], \tag{27}$$

$$0 = \bar{p}_G - \bar{\rho}\Omega_k^2\Delta_z^2 + \frac{1}{4\pi R^2\delta_R^2}\bar{\psi}_*\left[\frac{d^2}{dR_*^2}\bar{\psi}_G + \left(I_0'\right)^2\left(\bar{\psi}_G + \psi_z\right)\right]. \tag{28}$$

III. THE MASTER EQUATION AND COMPOSITE DISK STRUCTURES

The analysis of the disk structures, that can be formed in the vicinity of compact objects such as black holes leads to conclude that these are composite structures. These are characterized by a "core" of highly ordered magnetic field configurations with relatively strong fields and a thermal "envelope" where the magnetic field does not play an important role. In fact, there is an increasing body of experimental observations [4] that supports the existence of composite structures around a broad variety of objects.

We observe that for a "conventional" thin disk configuration

$$\left|\frac{z}{R}\frac{\partial\rho}{\partial z}\right| \sim \left|\frac{\partial\rho}{\partial R}\right| \quad \text{and} \quad \frac{\partial}{\partial z} \gg \frac{\partial}{\partial R}.$$

On the other hand, for the configurations we shall consider

$$\frac{\partial}{\partial R} \gtrsim \frac{\partial}{\partial z} \gg \frac{1}{R} \quad \text{and} \quad I\frac{dI}{d\psi} \sim \Delta_*\psi \,. \tag{29}$$

In this case $\nabla^2 \simeq \partial^2/\partial R^2 + \partial^2/\partial z^2$ and the Master Equation (14) reduces to

$$\frac{\partial}{\partial z}\left[R\rho\left(\Omega^2 - \Omega_k^2\right)\right] + \Omega_k^2 z\frac{\partial}{\partial R}\rho + \frac{1}{4\pi}\left(B_z\nabla^2 B_R - B_R\nabla^2 B_z\right) \simeq 0\,, \tag{30}$$

that is independent of the toroidal field component.

In this connection we note that the derivation of the Master Equation is compatible with a pressure tensor of the form

$$\underline{\underline{P}} = p_{th}\underline{\underline{\mathbf{I}}} + p^F\mathbf{e}_\phi\mathbf{e}_\phi \tag{31}$$

where p^F indicates the anisotropic pressure of a fast particle population that may be present, $p_{th} = p_e + p_i$ and p_e and p_i are the electron and the ion thermal population pressure. As an illustrative case for which Eq. (30) ceases to be valid, we consider a pressure tensor with a superthermal electron population that can be represented as

$$\underline{\underline{P}} = \left(p_e + p_i\right)\underline{\underline{\mathbf{I}}} + p_e^F\mathbf{e}_R\mathbf{e}_R\,. \tag{32}$$

where $p_e^F\mathbf{e}_R\mathbf{e}_R$ is the main component of the pressure tensor associated with the superthermal electron population. In the theoretical model for the three plasma regimes considered in Section VIII we shall agree that a distribution of this kind may prevent an axisymmetric configuration to develop allowing instead the formation of tridimensional spirals whose excitation can be associated [6] with gradients of the plasma temperatures.

Referring to cases for which Eq. (30) is valid, we rewrite it as

$$2R_0\Omega_k\frac{\partial}{\partial z}\left[\rho\delta\Omega\left(\psi_1\right)\right] + \Omega_k^2 z\frac{\partial}{\partial R}\rho = \frac{1}{4\pi R_0^2}\left[\frac{\partial\psi_1}{\partial R}\left(\nabla^2\frac{\partial\psi_1}{\partial z}\right) - \frac{\partial\psi_1}{\partial z}\left(\nabla^2\frac{\partial\psi_1}{\partial R}\right)\right] \tag{33}$$

and we can separate this into the following two equations

$$R_0\Omega_D^2\bar{\rho}\frac{\bar{\psi}_*}{B_0R_0^2}=-\frac{1}{4\pi R_0^2\delta_R^3}\left[\frac{d\bar{\psi}_*}{dR_*}\frac{d^2\bar{\psi}_*}{dR_*^2}-\bar{\psi}_*\frac{d^3\bar{\psi}_*}{dR_*^3}\right], \tag{34}$$

$$R_0\Omega_D^2\left(\bar{\rho}\frac{\bar{\psi}_G}{B_0R_0^2}+\rho_G\frac{\bar{\psi}_*}{B_0R_0^2}\right)+\Delta_z^2\frac{\Omega_k^2}{\delta_R}\frac{d}{dR_*}\bar{\rho}$$
$$=-\frac{1}{4\pi R_0^2\delta_R^3}\left[\frac{d}{dR_*}\bar{\psi}_G\frac{d^2}{dR_*^2}\bar{\psi}_*-\bar{\psi}_*\frac{d^3}{dR_*^3}\bar{\psi}_G\right]. \tag{35}$$

Then we may introduce the normalization density ρ_N and define

$$D_*\left(R_*\right)\equiv\frac{\bar{\rho}}{\rho_N}\quad\text{and}\quad y_*\equiv\frac{\bar{\psi}_*}{\bar{\psi}_{*0}}.$$

Thus Eq. (34) becomes

$$D_*y_*=-\left(\frac{dy_*}{dR_*}\frac{d^2y_*}{dR_*^2}-y_*\frac{d^3y_*}{dR_*^3}\right), \tag{36}$$

for

$$\delta_R^3\equiv\frac{\bar{\psi}_{*0}B_0}{\left(4\pi\bar{\rho}_N\right)\Omega_D^2R_0}, \tag{37}$$

and if we write

$$\bar{\psi}_G\equiv B_0\Delta_z^2\frac{\Omega_k^2}{\Omega_D^2}\frac{R_0}{\delta_R}y_G\equiv\bar{\psi}_{G0}y_G, \tag{38}$$

Eq. (35) becomes

$$\varepsilon_GD_{*G}y_*+D_*y_G+\left(\frac{d}{dR_*}y_G\right)\left(\frac{d^2}{dR_*^2}y_*\right)-y_*\frac{d^3y_G}{dR_*^3}=-\frac{dD_*}{dR_*}. \tag{39}$$

Here

$$\varepsilon_GD_{*G}=\frac{\rho_G}{\rho_N}\varepsilon_0^0\frac{3\delta_RR_0}{\Delta_z^2},$$

$\varepsilon_GD_{*G}\ll1$ and

$$\varepsilon_0^0\equiv\frac{\bar{\psi}_{*0}}{B_0R_0^2}, \tag{40}$$

that we consider as not too small. Then we have, from Eq. (37),

$$\delta_R=\left(\frac{\bar{\psi}_{*0}^2}{4\pi\rho_N\Omega_D^2\varepsilon_0^0}\right)^{1/3}\frac{1}{R_0}. \tag{41}$$

Now we consider ρ_G to be localized over a scale distance Δ_H and in particular

$$\rho_G=\bar{\rho}_G\left(R_*\right)\exp\left(-\frac{z^2}{2\Delta_H^2}\right), \tag{42}$$

where $\Delta_H^2\gg\Delta_z^2$. Then we may take

$$\psi_G \simeq \bar{\psi}_G(R_*)\exp\left(-\frac{z^2}{4\Delta_H^2}\right), \tag{43}$$

and refer to Eq. (33) obtaining

$$\Omega_k^2 \frac{z}{\delta_R}\frac{d}{dR_*}\bar{\rho}_G \simeq \frac{1}{4\pi R_0^2 \delta_R^3}\left\{\left(\frac{d}{dR_*}\bar{\psi}_G\right)\left(\frac{d^2\bar{\psi}_G}{dR_*^2}\right)\left(-\frac{z}{2\Delta_H^2}\right)+\left(\frac{z}{2\Delta_H^2}\right)\bar{\psi}_G\frac{d^3\bar{\psi}_G}{dR_*^3}\right\}. \tag{44}$$

Using the dimensionless quantities introduced earlier, this reduces to

$$\frac{d}{dR_*}D_{*G} \simeq \frac{1}{2}\left[\left(\frac{d^3 y_G}{dR_*^3}\right)y_G - \left(\frac{dy_G}{dR_*}\right)\frac{d^2 y_G}{dR_*^2}\right], \tag{45}$$

for

$$\Delta_H^2 = \frac{\Delta_z^2}{\varepsilon_G}. \tag{46}$$

IV. SIMPLE SOLUTIONS

A relatively simple family of solutions that generalizes that given in Ref. [5] is found for

$$D_* = D_N \frac{\sin^2 R_*}{1+\varepsilon_* \cos R_*}, \tag{47}$$

where ε_* is a positive parameter with $\varepsilon_* \lesssim 1/4$. Correspondingly,

$$y_* = \frac{2}{3\varepsilon_*}D_N\left[\sin R_* + \frac{\varepsilon_*}{2}\sin 2R_*\right]. \tag{48}$$

We note that for $D_N \to 0$, $\varepsilon_* \to 0$ Eq. (36) has the "homogenous" solution $y_* = 2D_N/(3\varepsilon_*)\sin R_*$. A representation of the surfaces $\alpha_z R_* - y_* = \text{const.}$, for $-\pi < R_* < \pi$, is given in Fig. 1.

Moreover, arguing that the contribution to $\bar{p}_{**}$ due to the plasmas currents should be of the order of $\left(\psi_{*0}/\delta_R R_0\right)^2 \varepsilon_*$ we may choose I_0' such that

$$\left(I_0'\right)^2 \simeq 1-\varepsilon_*^*.$$

Then

$$2\bar{p}_{**} - \frac{1}{4\pi R_0^2\delta_R^2}\bar{\psi}_{*0}^2\frac{3}{4}\varepsilon_*\sin^2 R_*\left(\frac{4}{3}\frac{\varepsilon_*^*}{\varepsilon_*}+\cos R_*\right) \simeq 0, \tag{49}$$

where $\varepsilon_*^* > (3/4)\varepsilon_*$.

Now we observe that if we consider only the innermost region $(z \le \Delta_z)$ the expression for the plasma temperature becomes

$$\frac{2T}{m_i} \simeq \frac{p_{**}(R_*)\exp\left(-z^2/\Delta_z^2\right)+\bar{p}_G(R_*)\exp\left[-z^2/\left(2\Delta_z^2\right)\right]}{\bar{\rho}(R_*)\exp\left[-z^2/\left(2\Delta_z^2\right)\right]+\bar{\rho}_G(R_*)}. \tag{50}$$

Next we refer to Eq. (39) and considering $\varepsilon_*^2 \ll 1$ we obtain

$$y_G = y_G^0 \sin R_* + y_{G1} \tag{51}$$

with

$$y_{G1}''' + y_{G1}' \simeq \varepsilon_G D_{*G} + \frac{3}{8}\varepsilon_* y_G^0\left[1-3\cos\left(2R_*\right)\right]+3\varepsilon_*\cos R_*. \tag{52}$$

Then the combination of Eq. (45), (51) and (52) suggests we take $\left|y_G^0\right| \sim \varepsilon_*^{-1/2}$, as this is consistent with $D_{*G} \sim 1$, and $\varepsilon_G \sim \varepsilon_* \left|y_G^0\right| 3/8$.

Clearly, as indicated by the expression for D_*, the core of the composite structure consists of a sequence of plasma rings. In this context, we note that the resolved X-ray emission from the Crab nebula by the Chandra space telescope [19] have revealed the existence of a sequence of concentric plasma rings around the relevant pulsar. We observe also that the ballooning modes that are found in the linear approximation, to be excited from a currentless disk can involve a doubly peaked density profile [20] represented by

$$\tilde{\rho} \propto z^2 \exp\left(-\sigma\frac{z^2}{2}\right). \tag{53}$$

Therefore, it is worth investigating whether these may evolve into a non linear configuration with rings at different heights along the z-axis that are reminiscent of the rings appearing in the Chandra X-ray image [19] of the Vela pulsar. It is evident at this point that a more complete analysis of the Master Equation requires a parallel computational approach.

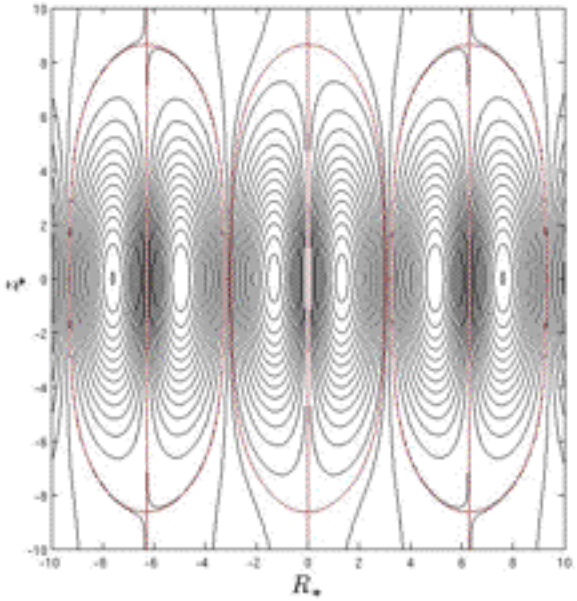

FIG. 1. Closed and open magnetic surfaces in the core of a composite disk structure.

V. Accretion Paradox

Now we consider the issues that arise when a radial accretion [9,10,11] velocity $\mathrm{V}_R(R, z)$ is introduced into a generic magnetized disk structure. This can be estimated from the mass accretion rate $\dot{M}$ as

$$4\pi R\int_0^{H_\infty} dz\rho(R, z)\mathrm{V}_R(R, z) = \dot{M}(R),$$

where H_∞ denotes the height of the disk structure. Under strictly stationary conditions $\left(\partial A_\phi/\partial t = 0\right)$ and in an axisymmetric configuration, the toroidal electric field E_ϕ has to vanish. Then, considering the simplified electron momentum conservation equation $-en\left(\mathbf{E}+\mathbf{V}\times\mathbf{B}/c\right)-\nu_{ei}m_e n\left(\mathbf{u}_e-\mathbf{u}_i\right)\simeq 0$ the allowed radial velocity is

$$\mathrm{V}_R \simeq D_m\frac{1}{B_z}\left(\frac{\partial}{\partial R}B_z-\frac{\partial}{\partial z}B_R\right) \tag{54}$$

where $D_m = \nu_{ei}c^2/\omega_{pe}^2$ and ν_{ei} is the electron-ion momentum transfer rate. Thus $\mathrm{V}_R \sim D_m/R$ and if we take the collisional (classical) value for ν_{ei}, we have

$$D_m^{cl} \simeq 4\times 10^{-2}\left(\frac{1\ \mathrm{keV}}{T_e}\right)^{3/2}\left(\frac{\ln\Lambda}{15}\right)\ \mathrm{cm}^2/\mathrm{s}. \tag{55}$$

It is evident that D_m^{cl}/R is unrealistically low to justify the needed accretion velocities. Therefore, an assumption that is frequently made is that ν_{ei} is strongly anomalous that is, larger than its classical value by many orders of magnitudes. In fact, a microinstability, for instance driven by the electron drift velocity, that could produce the needed kind of enhancement is most difficult to envision as the required current density would need to have unrealistically high values. Another important issue is that a process for a consistent rate of outward transport of angular momentum needs to be present.

VI. Bursty Accretion

The resolution of the "accretion paradox" that is proposed is based on assuming that a coherent composite structure of the type described in Section III is formed and that the plasma flow is guided by the magnetic field configuration over nearly all of the disk structure. The occurrence of this flow requires the presence of a finer scale angular momentum transport process of contrary direction. In particular: i) the total flow velocity $\mathbf{V}$ complies with the frozen in condition

$$\mathbf{V} = \alpha_{\mathrm{v}}\mathbf{B}_p + \Omega(\psi)R\mathbf{e}_\phi, \tag{56}$$

if we assume for simplicity that $B_\phi = 0$, by following successive separatrices as indicated in Fig. 2; ii) the plasma is carried from one separatrix to the next by the onset of ballooning modes that are driven by a difference between the gravitational and the centrifugal acceleration; iii) the result is a form of "modulated accretion"

associated with the onset of the considered modes and their decay, due to the depletion of the accumulated plasma of the considered modes.

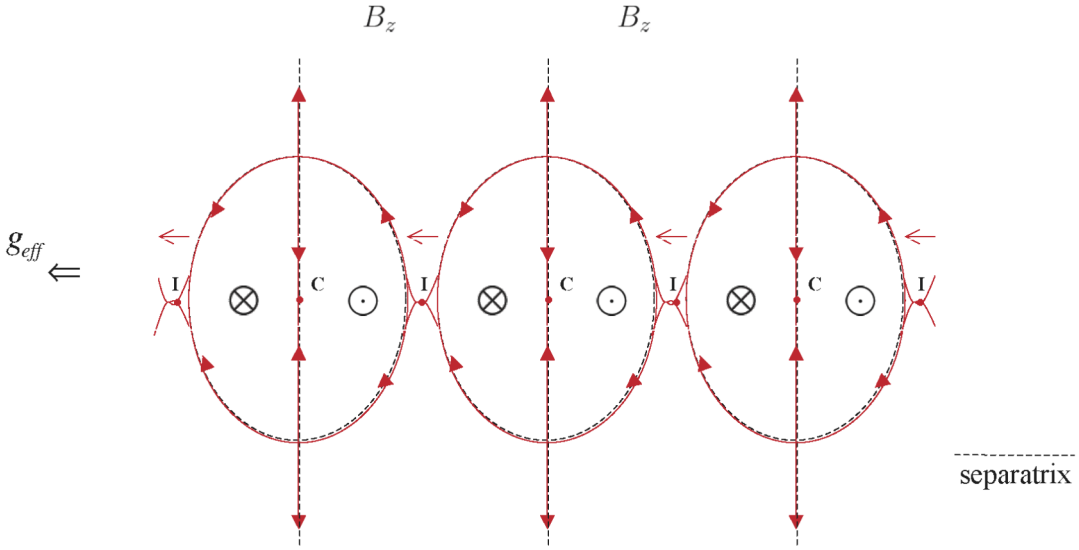

FIG. 2. Plasma flow patterns according to the Bursty Accretion scenario.

The process that we envision is very similar to that involved in the commonly observed Edge Localized Modes (ELMs) in magnetically confined plasmas. In this case ballooning modes associated with the effects of the plasma pressure gradient at the outer edge of the plasma column are considered to be responsible for the periodic bursts of particles and thermal energy unloaded on the surrounding material wall. As in the case of ELMs the instability growth rate is expected to evolve after the mode onset until most of the density accumulated on one separatrix is unloaded onto the next. Thus accretion proceeds in spurts, populating successive rings until it reaches the innermost plasmas regions that are considered to surround a black hole

This scenario can justify the experimental observation that "inactive" massive black holes at the center of galaxies are more frequent in older galaxies that should have suffered collisions. Thus we argue that coherent magnetic structures of the kind needed for the occurrence of accretion could not survive. Moreover, the result of the envisioned modulated accretion is that successive plasma rings are carried toward the black hole and can be ejected in opposite vertical directions depending on the direction of the toroidal currents flowing in them as shown in Fig. 3. Consequently, jets [21,22] can be envisioned as a well collimated vertical sequence of "smoke-rings" originating from the inner element of a composite disk structure.

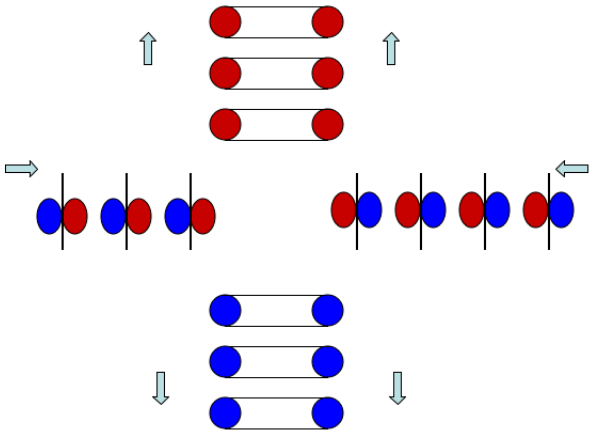

FIG. 3. Ring ejection scenario.

The modes that can provide the plasma unloading from one separatrix to the next are tri-dimensional with a high toroidal number m_ϕ. The relevant density perturbation can be described as

$$\hat{n} \simeq \tilde{n}(\ell)\exp\left[-i\omega t + ik_R\left(R - R_0\right) + im_\phi\phi\right] \tag{57}$$

where $\omega = m_\phi\Omega\left(R_0\right) + i\gamma_0$ and ℓ indicates a distance from the equatorial plane along the magnetic field lines. These modes co-rotate with the plasma at $R = R_0$ and we assume that

$$\gamma_0 > m_\phi \frac{d\Omega}{dR}\left(R - R_0\right). \tag{58}$$

Since these modes can be localized around $z = 0$ we may assume that the local magnetic field is nearly in the z direction and consider the plasma to have a finite electrical resistivity η. The relevant magnetic diffusion coefficient is $D_m = \eta c^2/4\pi$ and the plasma will be allowed, locally, to slip through the magnetic field [13] for sufficiently high values of $k_\perp$ that

$$\gamma \lesssim k_\perp^2 D_m. \tag{59}$$

Here

$$k_\perp^2 \simeq k_R^2 + \frac{m_\phi^2}{R_0^2}.$$

A corresponding process for the outward transport of angular momentum needs to be identified.

VII. GENERAL RELATIVITY CORRECTIONS

The phenomena we consider to guide the presented theory, such as High Frequency Quasi Periodic Oscillations (HFQPOs) [23,24], are estimated [25] to be related to processes taking place at distances $R \gtrsim 10R_G$, where $R_G \equiv GM_*/c^2$. Therefore, we can extend the theory given in the previous sections by adopting effective gravitational potentials that include General Relativity effects and can be justified for these distances. In particular, when considering a non-rotating black hole we use the Paczynsky-Wiita [26] gravitational potential

$$\phi_G \simeq -\frac{GM_*}{R-2R_G}. \tag{60}$$

It is easy to verify that this gives the correct radius (also known as ISCO) for the marginally stable orbit ($R_{MS} = 6R_G$), that the rotation frequency is

$$\Omega_G \simeq \frac{1}{R-2R_G}\left(\frac{GM_*}{R}\right)^{1/2}, \tag{61}$$

and

$$\Omega_D^2 = -\frac{Rd\Omega_G^2}{dR} = \frac{3R-2R_G}{R-2R_G}\Omega_G^2. \tag{62}$$

As pointed out earlier Ω_D^2 has a prominent role in Eqs. (34) and (35) and is one of the driving factors of the spectrum of modes [6] that can lead to the formation of a ring sequence configuration. As we can see, Ω_G is increased by a factor $3/2$ and Ω_D^2 by a factor 3 for $R = 6R_G$ relative to the Newtonian values.

We observe that, numerically, $R_G \simeq 14.8\left[M_*/(10M_\odot)\right]$ km and $R_{MS} \simeq 89$ $\left[M/(10M_\odot)\right]$ km. Considering a disk structure whose height is $2H$, at a given radius $R \gg R_G$, and a mass accretion rate $\dot{M}$ about $10^{-9}\,M_\odot/\mathrm{yr}$, a rudimentary estimate of the plasma density may be made by an average mass conservation equation like $\simeq 2\left[\bar{\bar{M}}/\bar{\bar{H}}\bar{\bar{R}}\right]\times\left[5kms^{-1}/\bar{V}_R\right]\times 10^{17}\,\mathrm{cm}^{-3}$ where $\bar{\bar{M}} = \dot{M}/\left(10^{-9}\,M_\odot/\mathrm{yr}\right)$, $\bar{\bar{H}} = H/\left(10^3\ \mathrm{km}\right)$, $\bar{\bar{R}} = R/\left(10^4\ \mathrm{km}\right)$. The corresponding Keplerian velocity is $\mathrm{V}_\phi = c\left(R_G/R\right)^{1/2} \simeq 1.2\times 10^4\left(\bar{\bar{M}}/\bar{\bar{R}}\right)^{1/2}$ km s^{-1} where $\bar{\bar{M}} = M_*/(10M_\odot)$.

We note that the radius R_{MS} depends in a significant way on the value of the angular momentum $\mathbf{J} = J\mathbf{e}_z$ that a black hole can have [15]. This is characterized by the dimensionless parameter

$$a_* = \frac{J}{M_* c R_G} \tag{63}$$

with $0 < a_* < 1$, $a_* \to 1$ being the so-called "extreme Kerr" limit. When $a_* \to 1$, $R_{MS} = R_G$ (for a direct orbit), $R_{MS} = 9R_G$ (for a retrograde orbit) while $R_{MS} = 6R_G$ for $a_* = 0$, as indicated earlier. Another important radius associated with the Kerr metric

to consider is that of the Ergosphere on the equatorial plane $R_E^0 = 2R_G \equiv R_S$. As is well known, the Kerr metric is

$$ds^2 = -\left(1 - \frac{2R_G r}{r_a^2}\right)(cdt)^2 - (2F_K)(ad\phi)(cdt)$$

$$= \left(r^2 + a^2 + a^2 F_k\right)\sin^2\theta(d\phi)^2 + \frac{r_a^2}{\Delta_a^2}dr^2 + r_a^2(d\phi)^2, \qquad (64)$$

where Boyer-Lindquist coordinates are used, $r_a^2 \equiv r^2 + a^2\cos\theta$, $a \equiv a_* R_G = J/(M_* c)$, $\Delta_a^2 = r^2(1 - 2R_G/r) + a^2$ and $F_K = \left(2rR_G/r_a^2\right)\sin^2\theta$.

In this case we may consider the effective potential for particles orbits in the plane $z = 0$, whose radial velocity is given by $\dot{R}^2/(2c^2) + \mathrm{V}_{eff}(R, E_N, L) = E_N/c^2 = \mathcal{E}$, where

$$\mathrm{V}_{eff} = -\frac{R_G}{R} + \frac{L^2/c^2 - 2a^2\mathcal{E}}{2R^2} - \frac{R_G}{R^3}\left(\frac{L}{c} - a\sqrt{\mathcal{E}+1}\right)^2 \qquad (65)$$

and L is the particle specific angular momentum. For circular orbits $\mathrm{V}_{eff} = \mathcal{E}$ and $d\mathrm{V}_{eff}/dR = 0$, give $\mathcal{E}$ and L as functions of R. Then the radius R_{MS} is obtained from $d^2\mathrm{V}_{eff}/dR^2 = 0$. As can be verified, when $a_* = 0$ the values of L and associated Ω are relatively close, numerically, to those obtained from Eq. (60). In particular, we may adopt Eq. (65) to add General Relativity corrections [15] to the relevant theory developed in the Newtonian limit.

VIII. Plasma Regimes And Regions

Now, taking into account the characteristics of the observed radiation emission from black hole candidates, we may envision a sequence of three plasma regions developing in the vicinity of a rotating and "active" black hole. These regions differ by the kinds of plasma and magnetic field geometry that are present in them. In particular, we consider

i) a "Buffer Region"
ii) a "Three-regime Region"
iii) a "Structured Low Temperature Region"

The Buffer Region is assumed to be bounded by the Ergosphere and to extend to a distance close to the radius of the marginally stable (e.g. $R_{MS} \simeq 9R_G$) retrograde orbit. This region is assumed to be strongly turbulent. Thus coherent structures originating from external regions should remain excluded from it. The source of energy for this region is considered to be the rotational energy of the black hole [27].

In the region surrounding to the Buffer Region three plasma regimes can emerge (see Fig. 4). Each regime is characterized both by different particle distributions in velocity space and by different coherent plasma structures. In particular, we may identify

a) an "Extreme" (highly non thermal) Regime in which spiral structures are excited.

b) an "Intermediate Non-thermal" Regime in which plasma ring structures are present and rings are ejected vertically at the inner edge of the region.

c) a "Dissipative Thermal" regime where the ring structure is gradually dissipated within the Region before reaching the Buffer Region.

In fact, it is well established experimentally, on the basis of the characteristics of the radiation emitted from Binary Black Holes [2] that these can be attributed to 3 states: i) a "Steep Power Law" (SPL) State, ii) a "Hard" State, iii) a Thermal State. Transitions between states have been observed for the same object.

In particular,

a) Referring to the "Extreme Regime" the assumption made in the derivation of the Master Equation that the electron distribution is represented by a scalar pressure p_e can no longer be made. In particular, if the pressure tensor has an anisotropy of the type represented by Eq. (32) the Master Equation (30) is no longer valid and we may argue that a two dimensional configuration of a disk structure may not be established. Then dual spiral structures with the same basic characteristics as those described in Ref. [6] are envisioned to become dominant. These consist of two spiral channels, one with a relatively high plasma density and one with a low density. The existence of the low density region characterized by relatively low runaway critical fields is consistent with the onset of spiral structures represented by the following density profiles

$$\hat{n} \simeq \tilde{n}_0^0 \frac{z}{\Delta_L^0} \exp\left[-\frac{\left(R-R_2\right)^2}{\Delta_R^2} - \frac{z^2}{\left(\Delta_L^0\right)^2} \right] \sin\left\{ k_R\left(R-R_L\right) - m_\phi\left[\Omega\left(R_L\right)-\phi\right]\right\}. \quad (66)$$

Here R_L is the radial distance around which the mode is localized, Δ_R and Δ_L^0 are the radial and vertical localization distances, respectively, $\Omega\left(R_L\right)$ is the frequency of the plasma rotation around the black hole, and m_ϕ/R_L and k_R are the toroidal and radial mode numbers, respectively. Moreover, $\mathrm{sgn}\left(k_R m_\phi\, d\Omega/dR\right) < 0$ corresponding to trailing spirals.

We note that the expressions for k_R, Δ_R, and Δ_L^0 found from the linearized theory [6] are $k_R \simeq k_0 = \Omega_D/\mathrm{v}_A$, $\mathrm{v}_A^2 = B_0^2/\left(4\pi\rho_0\right)$, where B_0 is the vertical

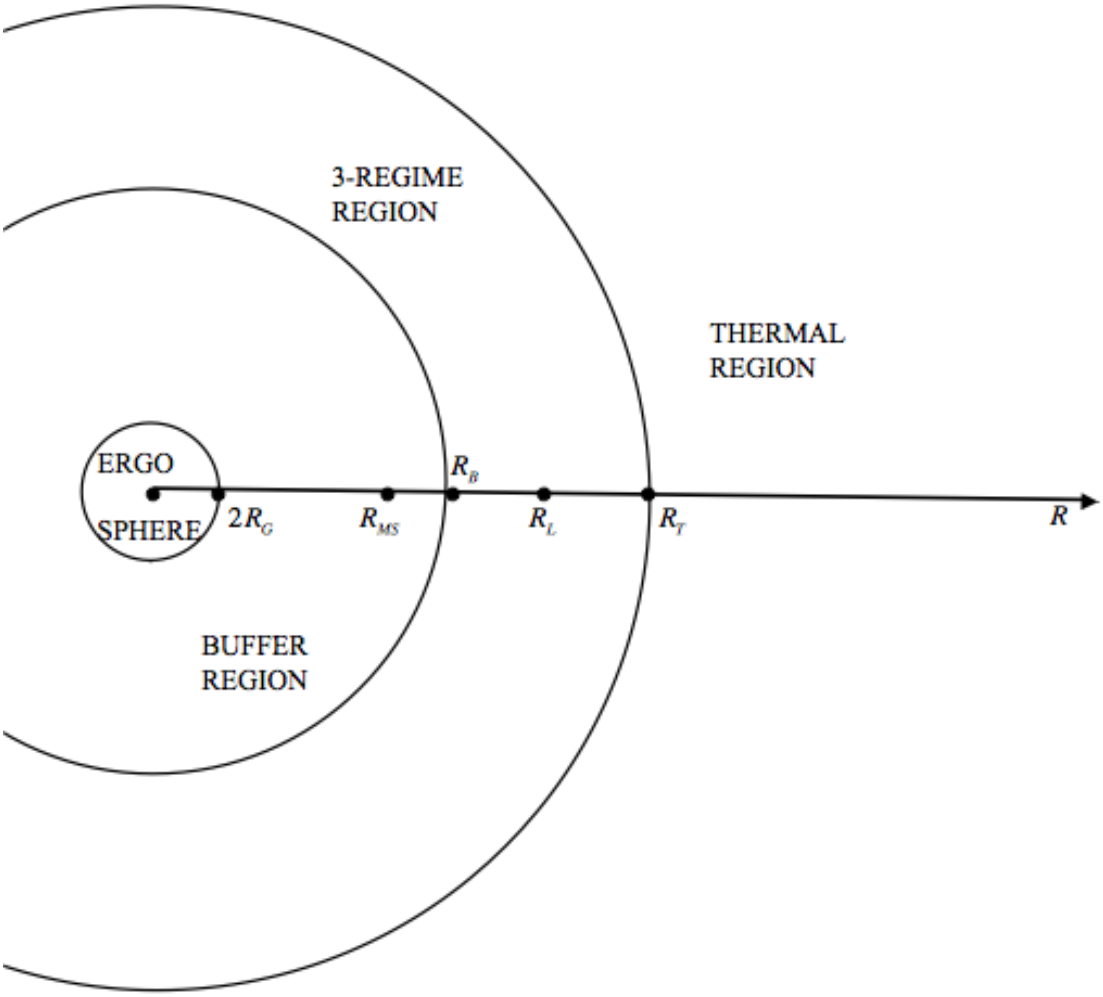

FIG. 4. Sketch in the equatorial plane of the plasma regions surrounding a rotating black hole. Here $R_{MS} = 9R_G$ and R_L is the distance at which the maximum amplitude of the spiral modes is localized.

"seed" magnetic field from which the considered perturbation can emerge, ρ_0 is the plasma density on the equatorial plane, $\Delta_L^0 \simeq \left(H_0/k_0\right)^{1/2}$,

$$\Delta_R \simeq \left\{ \frac{\gamma_0}{\left|\frac{d\Omega}{dR}\right| m_\phi k_R} \right\}^{1/2} \sim \left(\frac{\gamma_0 R_L}{\Omega_k k_0 m_\phi} \right)^{1/2}, \tag{67}$$

γ_0 is the linear growth rate of the unstable mode, $\gamma_0 < \Omega$, $H_0 \equiv c_s/\Omega_k\left(R_L\right)$ and c_s is the local velocity of sound. We observe that accretion should be allowed to proceed at relatively fast rates along the considered spiral structures.

Then we may estimate the spiral co-rotational radius to be at the distance $R_L \simeq \alpha_{MS} R_{MS} + \Delta_R^0$ where $R_{MS} \simeq 9R_G$, and α_{MS} is an appropriate uncertainty

parameter. In addition, we may estimate Δ_R^0 as $\Delta_R^0 \simeq \varepsilon_R \left(R_L H_0\right)^{1/2}$ where $\varepsilon_R < 1$ is a second uncertainty parameter.

We assume that the lowest harmonics $m_\phi = 2$, 3 prevail in the spiral non-linearly developed spectrum. Then we argue [25] that High Frequency Quasi Periodic Oscillations (HFQPO's) are associated with these modes and have frequencies $2\Omega\left(R_L\right)$ and $3\Omega\left(R_L\right)$, respectively, as observed experimentally. The values of $\Omega\left(R_L\right)$ that are observed from the experiments for a given black hole of mass M_* indicate that, typically, $R_L > 10R_G$. Therefore, the General Relativity corrections to the theory for the plasmas in this region are relatively modest [15].

b) When the particle distributions in momentum space have a non-thermal component such as that represented by Eq. (31) which allows the formation of a composite axisymmetric disk structure in the Three-regime Region, the excitation of spiral modes can be prevented. Then the associated HFQPOs disappear. In addition we may argue that as a result of the interaction between the composite disk structure and the strong turbulence at the edge of the Buffer Region the last couple of plasma rings, carrying oppositely directed toroidal plasma currents that repel each other, could be ejected vertically. Following the arguments given in Section VI the plasma rings can be expected to "arrive" intermittently with a period related to the onset of the modes that transfer particles from one separatrix to the next. In particular, we may envision that jets results from the ejection of toroids ("smoke-rings") carrying currents in the same (toroidal) directions launched in opposite vertical directions. We also note that experimental observations indicate that jets emerge from evolving disk structures.

In this connection we point out that a recent paper [28] suggests that the power associated with jets [29] is independent of the estimated angular momentum of the black holes with which they are connected. On the other hand it is reasonable to assume that the properties of the Buffer Region and of the plasmas contained in it depend on the black hole rotation. We point out also that the formation and ejection of jets with a purely toroidal magnetic field was proposed and analyzed in Ref. [30].

c) In the Dissipative Thermal regime the plasma can reach a relatively high temperature and maintain a thermal distribution as the coherent ring structure is dissipated before reaching the Buffer Region.

Finally, in the outermost region the plasma is considered to be relatively cold and in a well thermalized state. In this region a composite disk structure such as that described in Section III is assumed to be well established allowing the (accreting) plasma to flow along successive magnetic separatrices as proposed in Section VI.

IX. Concluding Remarks

Composite disk structures, in the surrounding of black holes, have been identified theoretically through a Master Equation of which a set of "ring solutions" have been obtained. These structures are assumed to emerge from the excitation of linearly unstable axisymmetric modes out of unstructured (conventional) thin disks.

Concepts and results derived from the analysis of magnetically confined laboratory plasmas have been used in the relevant theory.

Characteristic plasma regions that develop in the close vicinity of black holes are envisioned by considering the properties of the observed radiation emission from Binary Black Holes and the evolution of theoretically identified magnetic field structures. In particular, the plasmas that are formed in one of these regions can exhibit three different regimes where different kinds of structures are associated with different kinds of spectra of X-ray radiation emission. This is consistent with the fact that, in general, the dynamics of high energy plasmas need a phase space (geometry and momentum) kind of description.

Clearly, there are numerous relevant issues that remain to be investigated. These include the process of extraction of black hole rotational energy in the context of the envisioned sequence of regions around the black hole, the non-linear description of spiral structures, the formation of highly collimated jets following the ejection of plasma rings proposed in Section VII, the origin of the non-thermal electron distributions in phase space producing the observed X-ray emission spectra, etc.

Acknowledgments

It is a pleasure to thank P. Rebusco for her advice and for sharing her knowledge of the characteristics of QPOs, R. Remillard for his guidance through the experimental observations on Binary Black Holes, T. Zhou for having suggested the parameter ε_* that generalizes the expression for D_*, and E. Gallo for her comments on galactic black holes. This work was sponsored in part by the U.S. Department of Energy.

Appendix A: Magnetic Fields Options for Rotating Plasma Disk Structures with Near Keplerian Frequencies.

We assume that, on a grand scale, the hyperconductivity condition $\mathbf{E}+\mathbf{V}\times\mathbf{B}/c=0$ can be applied and we consider an axisymmetric rotating plasma with $\mathrm{V}_\phi = R\Omega$ and

$$\Omega = \Omega_k(R) + \delta\Omega\,, \tag{A-1}$$

where $|\delta\Omega| < \Omega_k(R)$. The hyperconductivity condition implies that

$$\mathbf{V} = \alpha_{\mathrm{v}}\mathbf{B} + \omega_B(\psi)R\mathbf{e}_\phi\,. \tag{A-2}$$

Then

$$\left[\Omega_k(R)+\delta\Omega\right]R = \alpha_{\mathrm{v}}B_\phi + \omega_B(\psi)R\,, \tag{A-3}$$

where $\alpha_{\mathrm{v}} = \chi(\psi)/\rho$ from mass conservation, and we have several options such as:

i) $\alpha_{\mathrm{v}} = 0$ that means

$$\Omega_k(R) + \delta\Omega = \omega_B(\psi)\,. \tag{A-4}$$

In this case the magnetic surface ψ can only be a function of R to lowest order in $\delta\Omega/\Omega_k$. Therefore we take $\psi \simeq \psi_0(R) + \psi_1(R, z)$ and $\omega_B \simeq \omega_B^0(\psi_0) + \psi_1\left(d\omega_B^0/d\psi_0\right)$ with $\omega_B^0(\psi_0) = \Omega_k(R)$ and $\delta\Omega \simeq \psi_1\left(d\omega_B^0/d\psi_0\right)$. This is the option considered at the start of this paper and in earlier papers where the presence of an accretion velocity was neglected.

ii) $\alpha_v \neq 0$ with $B_\phi \neq 0$. Then

$$\Omega_k = \frac{\alpha_v}{R} B_\phi \ , \ \ \delta\Omega = \omega_B(\psi) + \frac{\delta\alpha_v}{R} B_\phi \ . \tag{A-5}$$

In this case there cannot be a poloidal field $\mathbf{B}_p$ without a corresponding velocity

$$\mathbf{V}_p \simeq \alpha_v \mathbf{B}_p \ .$$

Thus, if the considered poloidal velocities are smaller than V_ϕ, $|B_p| \ll B_\phi$.

iii) $\alpha_v \neq 0$ with $B_\phi = 0$. Then

$$\Omega_k + \delta\Omega = \omega_B(\psi) \tag{A-6}$$

as in the case of option i), and $\mathbf{V}_p = \alpha_v \mathbf{B}_p$. This is the option considered in Section VI.

Appendix B:
Currentless Thin Disk

The currentless Thin Disk is the closest plasma structure to that of the well known gaseous thin disk [9,10,11]. It is imbedded in a vertical magnetic field B_z, it has only a rotation velocity $V_\phi = \Omega R$ and is described by the vertical and horizontal equilibrium conditions

$$0 \simeq -\frac{\partial p}{\partial z} - \Omega_k^2 z\rho \ , \tag{B-1}$$

$$\rho\left(2\Omega_k \delta\Omega R + \frac{3}{2}\frac{z^2}{R}\Omega_k^2\right) \simeq -\frac{\partial p}{\partial R} \ , \tag{B-2}$$

where $\Omega \simeq \Omega_k(R) + \delta\Omega$. In this structure the Lorentz force due to internal currents is considered to be negligible. Therefore the expression for $\delta\Omega$ is relatively easy to evaluate and for the relevant components of $\mathbf{E}$ we refer to Section II.

Appendix C:
Numerical Estimates

Considering the Three-regime Region and the thermal regime in particular [2] if the plasma density is sufficiently high that the plasma is optically thick and its temperature is about 1 keV, the radiation emission can be estimated as

$$W_{BB} \simeq 10^{24} \ \text{erg/cm}^2 = 10^5 \ \text{MW/m}^2 \ .$$

The area of the two relevant surfaces is about (see Section VIII)

$$A_{TR} = 4\pi\Delta_R^0\left[R_{MS}\alpha_{MS} + \Delta_R^0\right]$$

Then, if we estimate $A_{TR} \simeq (1.5)^3 \times 10^{14}$ cm^2, $W_{BB}A_{TR} \simeq (1.5)^3 \times 10^{38}$ erg/sec is not far from the observed values.

The plasma density in this region may be evaluated, roughly, as follows

$$\bar{n}\,\bar{\mathrm{V}}_R/(5\,\mathrm{km/sec}) \simeq \frac{\dot{M}}{(10^{-9}\,M_\odot/\mathrm{yr})R/(150\ \mathrm{km})H/(40\ \mathrm{km})} \times 3\times 10^{20}\,\mathrm{cm}^{-3},$$

where for $\bar{\mathrm{V}}_R$ we may use a Shakura-Sunyaev [31] type of prescription, that is $\mathrm{V}_R \simeq \alpha_{ss} c_s H/R$ with $c_s \simeq 400$ km s^{-1}, $H/R \sim 1/4$ and $\alpha_{ss} \simeq 5\times 10^{-2}$.

REFERENCES

1. M. van der Klis, P. Murdin, *Encyclopedia of Astronomy and Astrophysics*, (Publ. Institute of Physics, London, 2000), 2380.
2. R.A. Remillard and J.E. McClintock, *Annu. Rev. A&A* **44**, 49 (2006).
3. D. Psaltis, ArXiv e-prints, 0806, 1531 (2008).
4. E.F. Taylor and J.A. Wheeler, *Exploring Black Holes* (Publ. Addison Wesley Longman, Boston, 2000), p. F-1.
5. B. Coppi and F. Rousseau, *Ap. J.* **641**, 458 (2006).
6. B. Coppi, *Astron. Astrophys.* **504**, 321 (2009).
7. B. Coppi, *Plasma Phys. Cont. Fus.* **51**, 124007 (8pp) (2009).
8. B. Coppi, *Plasmas in the Laboratory and in the Universe*, Eds. G. Bertin *et al.*, (Publ. *American Institute of Physics*, New York, 2010), p. 45.
9. D. Lynden-Bell, *Nature,* **223**, 690 (1969).
10. J.E. Pringle and M.J. Rees, *A&A,* **24**, 337 (1972).
11. J.E. Pringle, *Annu. Rev. Astron. Astrophys.* **19**, 137 (1981).
12. B. Coppi and M.N. Rosenbluth, Proc. 1965 *Int. Conf. on Plasma Physics and Controlled Nuclear Fusion Research (Vienna: IAEA)* Paper CN-21/106 (1965).
13. B. Basu and B. Coppi, *Geophys. Res. Lett.* **10** 900 (1983).
14. S. Kato, J. Fukue S. Mineshige, *Black-Hole Accretion* (Publ. Kyoto Univ. Press, Kyoto, 1998), p. 50.
15. J.B. Hartle, *Gravity,* (Publ. Addison Wesley, San Francisco, 2003), p.318.
16. G.I. Ogilvie, *M.N.R.A.S.* **888**, 63 (1997).
17. V.C.A. Ferraro, *M.N.R.A.S.* **97**, 288 (1987)
18. R. H. Cohen, B. Coppi and A, Treves, *Ap. J.* **179**, 269 (1973).
19. Chandra X-ray Observatory Center NASA/CXC/SAO. ACIA/HETG Image (2002).
20. B. Coppi and E.A. Keyes, *Ap. J.* **595**, 1000 (1996).
21. R.V.E. Lovelace, *Nature* **223**, 690 (1976).
22. R.D. Blandford, *M.N.R.A.S.* **176**, 465 (1976).
23. T.E. Strohmayer, W. Zhang, J.H. Swank, I. Lapidus, J.C. Lochner , *Ap. J.* **469**, p. L9 (1996).

24. M. van der Klis, R. Wijnands, W. Chen, F.K. Lamb, D. Psaltis, E. Kuulkers, W.H.G. Lewin, B. Vaughan, J. van Paradijs, S. Dieters, K. Horne, *IAU Circ.* **6424**, (1996).
25. B. Coppi and P. Rebusco, *E.P.S. Conf. on Plasma Physics (Crete, Greece)* Paper P5.154, (2008).
26. B. Pazcynsky and P.J. Wiita, *Astron. Astrophys*. **88**, 23 (1980).
27. R.A. Blandford and R.L. Znajek, *M.N.R.A.S.* **179,** 433 (1977).
28. R. P. Fender, E. Gallo and D. Russel, *M.N.R.A.S.* **406**, 1425–1434 (2010).
29. R.A. Blandford and D.G. Payne, *M.N.R.A.S.* **199**, 883 (1982).
30. J. Contopoulos, *Ap. J.* **45**, 616 (1995).
31. N.I. Shakura and R.A. Sunyaev, *Astron. Astrophys.* **24**, 337 (1973).